

# Polymer Nanocoating of Amorphous Drugs for Improving Stability, Dissolution, Powder Flow, and Tableability: The Case of Chitosan-Coated Indomethacin

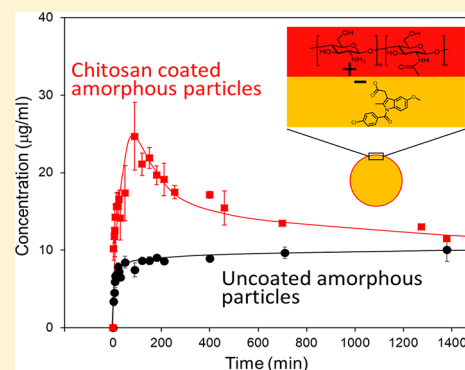
Yuhui Li,<sup>†</sup> Janguang Yu,<sup>†</sup> Shenye Hu,<sup>‡</sup> Zhenxuan Chen,<sup>†</sup> Mark Sacchetti,<sup>§</sup> Changquan Calvin Sun,<sup>‡</sup> and Lian Yu<sup>†,\*</sup>

<sup>†</sup>School of Pharmacy and <sup>§</sup>Zeeh Pharmaceutical Experiment Station, School of Pharmacy, University of Wisconsin-Madison, Madison, Wisconsin 53705, United States

<sup>‡</sup>College of Pharmacy, University of Minnesota, Minneapolis, Minnesota 55455, United States

## Supporting Information

**ABSTRACT:** As a result of its higher molecular mobility, the surface of an amorphous drug can grow crystals much more rapidly than the bulk, causing poor stability and slow dissolution of drug products. We show that a nanocoating of chitosan (a pharmaceutically acceptable polymer) can be deposited on the surface of amorphous indomethacin by electrostatic deposition, leading to significant improvement of physical stability, wetting by aqueous media, dissolution rate, powder flow, and tableability. The coating condition was chosen so that the positively charged polymer deposits on the negatively charged drug. Chitosan coating is superior to gelatin coating with respect to stability against crystallization and agglomeration of coated particles.



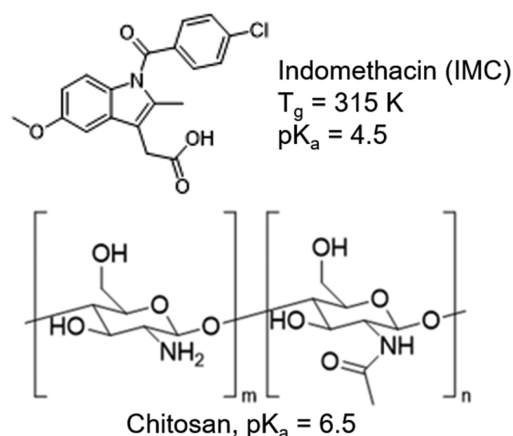
**KEYWORDS:** amorphous drug, surface coating, crystallization, dissolution, tableability, powder flow, indomethacin, chitosan

## INTRODUCTION

An active pharmaceutical ingredient can exist in many solid forms, both crystalline and amorphous. Amorphous formulations have attracted recent attention as a general method to improve the solubility and dissolution rate of poorly soluble drugs.<sup>1</sup> A key issue in this effort is the stability against crystallization, since amorphous drugs tend to crystallize over time, and crystallization would eliminate their advantages. Recent work has shown that molecular mobility can be extremely high on the free surface of amorphous drugs, and this leads to rapid crystal growth on the surface, while bulk crystal growth is relatively slow.<sup>2–4</sup> These results suggest that preventing surface crystallization is an efficient way to improve the stability of amorphous drugs.

Wu et al. showed that a nanocoating of polymers can effectively inhibit the surface crystallization of an amorphous drug as well as improve the powder flow.<sup>5</sup> Their coating process relied on electrostatic deposition, in which a polyelectrolyte deposits on an amorphous drug of the opposite charge. For indomethacin (IMC, Scheme 1, a weak acid with  $pK_a = 4.5$ ), coating was performed at  $pH = 5$ , at which the drug is negatively charged so that the polycation polydiallyldimethylammonium chloride (PDDA) can deposit on it. The polymer coating protects the drug against surface crystallization, because under the coating, surface molecules are immobilized. An attractive feature of this approach is that the coating can be

## Scheme 1. Molecular Structures of Indomethacin and Chitosan



extremely thin, on the order of several nanometers, since the neutralization of charges stops further deposition of charged polymer molecules. As a result, only a small amount of polymer

**Received:** November 26, 2018

**Revised:** January 11, 2019

**Accepted:** January 22, 2019

**Published:** January 22, 2019

is needed to significantly improve stability. This ability is useful for producing high-drug-loading formulations and for saving room in a formulation for other excipients needed to enhance disintegration and dissolution.

Because PDDA is not a pharmaceutical polymer, Teerakapibal et al. tested gelatin as a coating polymer.<sup>6</sup> Unlike PDDA, gelatin is a weak polyelectrolyte and not a homopolymer, having both acidic and basic amino acid segments. They found that a gelatin coating can offer similar protection against crystallization and that a gelatin coating is “forgiving” in that it does not require strict pairing of opposite charges. At a given pH, the amino acid segments in gelatin can be both positive and negative. As a result, gelatin–drug interactions are less well-defined as in the case of a homopolymer, with local variations according to amino acid segments.

The present study investigated the use of chitosan as a pharmaceutically acceptable coating material to replace PDDA and to improve upon gelatin as a coating polymer. Chitosan (Scheme 1) is a linear polysaccharide derived from chitin, whose chain segments are randomly distributed D-glucosamine and N-acetyl-D-glucosamine. The glucosamine group is weakly basic and protonated below pH  $\approx$  6.5 (the  $pK_a$  of chitosan),<sup>7</sup> making chitosan a polycation at low pH. Chitosan has been used as a polymer for electrostatic deposition to create ultrathin coatings (several nanometers for each chitosan layer).<sup>8</sup> From the  $pK_a$  values of chitosan (6.5) and IMC (4.5), we expect that in the pH range of 4.5–6.5, IMC is negatively charged, and chitosan is positively charged, enabling coating by electrostatic deposition. This hypothesis will be tested here. Since chitosan has lower charge density than PDDA when ionized (owing to partial amide formation), it is of interest to compare their performance in inhibiting crystallization. We report that the principle of electrostatic deposition can be extended to the chitosan–IMC system. The polycation chitosan can be deposited on the negatively charged IMC to suppress surface crystallization, and the resulting material shows significant improvement in dissolution rate, powder flow, and tabletability relative to uncoated IMC. We find that chitosan is superior to gelatin for coating amorphous IMC with respect to stability against crystallization and agglomeration of coated particles.

## MATERIALS AND METHODS

Indomethacin [1-(*p*-chlorobenzoyl)-5-methoxy-2-methylindole-3-acetic acid,  $\geq$ 99%, IMC], chitosan (medium molecular weight grade, MW  $\approx$  190–310 kg/mol), gelatin from porcine skin (Type A,  $\sim$ 300 bloom, MW = 50–100 kg/mol), and gelatin from bovine skin (Type B,  $\sim$ 225 bloom, MW = 50–100 kg/mol) were purchased from Sigma-Aldrich (St. Louis, MO) and used as received. Chitosan was dissolved in 0.3 wt % acetic acid (prepared by dissolving  $\geq$ 99.7% pure acetic acid purchased from Sigma-Aldrich in Milli-Q water) at a concentration of 2 mg/mL. The solution pH was adjusted to 5 by adding 1 M NaOH, which increased the solution volume by  $\sim$ 4%.

An amorphous IMC film with an open surface was prepared by melting 5 mg of the as-received crystalline material at 190 °C for 1 min between two microscope coverslips, cooling to room temperature, and gently removing one coverslip. To form a protective coating, the sample with a free surface was dipped in a chitosan solution for 10 s, dried with an absorbent tissue, and further dried at 295 K under vacuum for 3 h. To

prepare chitosan or gelatin-coated amorphous particles, 1 g of crystalline IMC was melted and cooled to room temperature to make a bulk glass. The bulk glass was broken into particles in the presence of 2 mL of coating solution using four methods: Retsch mill, vortex, magnetic stirrer, and homogenizer. In the Retsch mill method (MM 301, Retsch Inc., Newtown, PA), amorphous chunks were poured into a 20 mL metal tube together with 11 steel balls (5 mm). Particles were collected after milling for 75 s at a frequency of 25 Hz. In the vortex method, amorphous chunks were poured into a 20 mL glass vial containing two half inch steel balls. Particles were collected after milling for 60 s at the intensity scale of 7 using a vortex (S8223, Scientific Industries Inc., Bohemia, NY). In the magnetic stirrer method, amorphous chunks were poured into a 20 mL glass vial together with one 2.5 cm stir bar, and the vial was placed on its side on a stir plate. Particles were collected after stirring for 4 min at a speed of 100 rpm. In the homogenizer method (Polytron PT 1200 E, Kinematica AG, Switzerland), amorphous chunks were placed in a 10 mL glass beaker. Particles were collected after milling for 60 s with the homogenizer probe operating at 180 rpm. During the coating process, the pH of the coating solution did not change significantly ( $<0.01$ ). With each method, after particle size reduction, the slurry was filtered and dried at room temperature under vacuum for 3 h. As control, uncoated particles were also prepared by the homogenizer method but in the absence of a coating solution. Particle size distributions were determined by dispersing the particles in an immersion medium for microscopy and measuring their sizes through a light microscope (Nikon Optiphot Pol 2 equipped with a digital camera).

For crystallization studies, the temperature was maintained by ovens to  $\pm 1$  °C. Two levels of relative humidity (RH) were used: (1) 75% RH maintained by a saturated NaCl solution and (2) a “dry” condition (0–5% RH) maintained by storage in a desiccator loaded with Drierite. The stability test was performed under three conditions: 40 °C/dry, 40 °C/75% RH, and 30 °C/75% RH. The degree of crystallinity was calculated from the XRD patterns using

$$\text{crystallinity (\%)} = A_{\text{cryst}}/A_{\text{total}} \times 100$$

where  $A_{\text{cryst}}$  is the area of the crystalline peaks in an XRD pattern, and  $A_{\text{total}}$  is the total area of the crystalline peaks and the amorphous halo. The XRD patterns were integrated using the program EVA from Bruker-AXS.

X-ray powder diffraction (XRD) was performed with a Bruker D8 Advance X-ray diffractometer, which was equipped with a Cu K $\alpha$  source ( $\lambda = 1.54056$  Å) operating at a tube load of 40 kV and 40 mA. Each sample was scanned between 2 and 40° (2 $\theta$ ) with a step size of 0.02° and a maximum scan rate of 3 s/step. Samples of small quantity were analyzed on a Si (510) zero-background holder.

The dissolution rate of IMC particles was measured at 37 °C. Uncoated and chitosan-coated amorphous particles were prepared using the homogenizer method and tested immediately. IMC crystalline particles ( $\gamma$  polymorph as confirmed by XRD) were obtained by crystallizing uncoated amorphous particles under the 40 °C/dry condition. All the samples were sieved, and the 45–100  $\mu$ m sieve cut was used. After equilibrating 25 mg of particles in a dry dissolution vessel at 37 °C, 100 mL of Milli-Q water prewarmed to 37 °C was poured into the vessel. The mixture was stirred at a paddle speed of 150 rpm. At each time point, 2 mL of solution was

withdrawn from the vessel and replaced with 2 mL of Milli-Q water at 37 °C. The withdrawn solution was filtered through a 0.2  $\mu\text{m}$  membrane filter, and its concentration was determined by UV–vis spectrometry (8453, Agilent Technologies, Inc.) at 318 nm against a standard curve obtained by measuring IMC solutions of known concentrations. Each dissolution profile (concentration versus time) was the average of at least three samples.

To measure the angle of repose, 200 mg of IMC powder in the 45–100  $\mu\text{m}$  sieve cut was poured through a funnel whose outlet (3 mm inside diameter) was placed 0.5" above a horizontal receiving surface. A picture was taken of the rested powder from its side, and the angle of repose was measured from the image. Powder flowability was measured using a ring shear tester (RST-XS; Dietmar Schulze, Wolfenbüttel, Germany) at a preshear normal stress of 1 kPa under ambient conditions (23 °C and 50–55% RH). A 10 mL shear cell was used, and the measurement was made in triplicate. The normal stresses for shear testing were applied in the order 230, 400, 550, 700, 850, and back to 230 Pa. Data were analyzed using standard methods.<sup>9</sup> Unconfined yield strength ( $f_c$ ) and major principal stress ( $\sigma_n$ ) were obtained from each yield locus by drawing Mohr's circles. The flowability index,  $ff_c$ , was calculated using eq 1

$$ff_c = \frac{\sigma_n}{f_c} \quad (1)$$

For tabletability assessment, approximately 100 mg of powder was manually filled into a 6 mm diameter die and compressed using flat-faced punches on a Universal Material Testing Machine (model 1485; Zwick/Roell, Ulm, Germany) at a speed of 5 mm/min. Tablets were allowed to relax under ambient conditions for 24 h before their diameters, thicknesses, and weights were measured. Care was taken to remove the flashing before measuring tablet thickness.<sup>10</sup> The diametrical breaking force was then measured using a texture analyzer (TA-XT2i; Texture Technologies Corporation, Scarsdale, New York) at a speed of 0.01 mm/s. Tablet tensile strength was calculated from the maximum breaking force and tablet dimensions using eq 2<sup>11</sup>

$$\sigma = \frac{2F}{10^6 \pi DT} \quad (2)$$

where  $\sigma$  is tensile strength (MPa),  $F$  is the breaking force (N),  $D$  is the tablet diameter (m), and  $T$  is the tablet thickness (m). Each tabletability profile is a plot of tensile strength vs compaction pressure.

## RESULTS AND DISCUSSION

**Stability Test in Film Geometry.** The stability of chitosan-coated amorphous IMC was first tested in the film geometry. As shown in Figure 1a, without coating, significant crystallization occurred in 20 days. The crystals were opaque regions in an otherwise transparent amorphous film of light yellow color. In contrast, a chitosan-coated film remained amorphous under the same condition, indicating the ability of a chitosan coating to inhibit surface crystallization. Furthermore, the growth of pre-existing crystals with and without coating was followed. The pre-existing crystals were formed by annealing an open-surface sample for 3 to 4 days. These partially crystallized samples were then split into two groups: the first group was uncoated control; the second group was

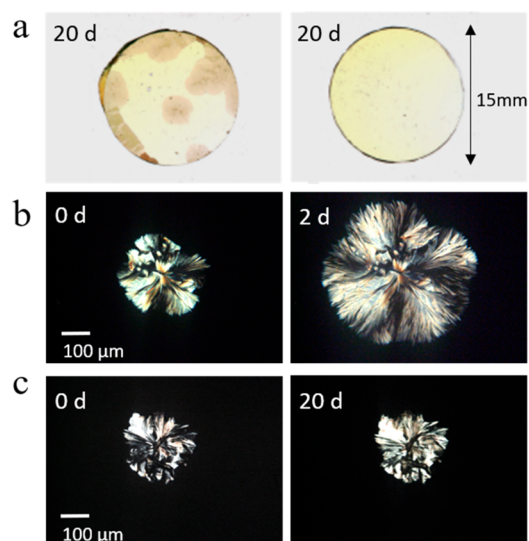


**Figure 1.** Effect of chitosan coating on surface crystal growth in an amorphous IMC film at 40 °C. Without coating (panel a, left), crystallization is evident in 20 days; with a chitosan coating (panel a, right), no crystallization is observed after 20 days. The as-prepared film was free of crystals (like the one on the right). Each film was prepared on a round glass coverslip (15 mm in diameter). (b) Progress of crystal growth in an uncoated film viewed through a microscope. Obvious growth is seen in 2 days. (c) Same as (b), except that the film is coated with chitosan. No significant growth is seen in 20 days.

coated to evaluate the effect of coating. Without coating, crystal growth was evident in 2 days at 40 °C (Figure 1b); the growth rate was  $0.7 \pm 0.1$  nm/s ( $n = 5$ ) in the  $\gamma$  polymorph, consistent with the previous report.<sup>12</sup> In contrast, under a chitosan coating, no growth was detected even after 20 days (Figure 1c).

**Stability of Coated Amorphous Particles.** In addition to coated films, the effect of chitosan coating on the surface crystallization of amorphous particles was studied. All coated particles were prepared with the homogenizer method (see Materials and Methods), which as we discuss below, is superior to the other methods under the conditions tested. The coated particles were tens of micrometers in size (Figure S1), and their size distribution was similar to that of the uncoated particles, consistent with the small thickness of the coating and the absence of coating-induced granulation. Figure 2 shows the typical XRD data for testing physical stability. XRD patterns are compared for uncoated and coated particles at 30 °C and 75% RH. The uncoated particles show significant crystallization, while coated particles remain amorphous, indicating improved stability.

Figure 3 compares the change of crystallinity of amorphous particles coated with chitosan and gelatin (Type A and B) under three different conditions: 40 °C/dry, 40 °C/75% RH, and 30 °C/75% RH. Under all the conditions tested, coated particles were more resistant to crystallization than uncoated particles. At 40 °C (Figure 3a), the chitosan coating performed significantly better than the gelatin coating (A or B). The same is true at 40 °C and 75% RH (Figure 3b). At 30 °C and 75% RH, chitosan and gelatin coatings had similar performance in suppressing crystallization (Figure 3c). Overall, chitosan outperformed gelatin as a coating material for inhibiting crystallization. This could be a result of the higher charge

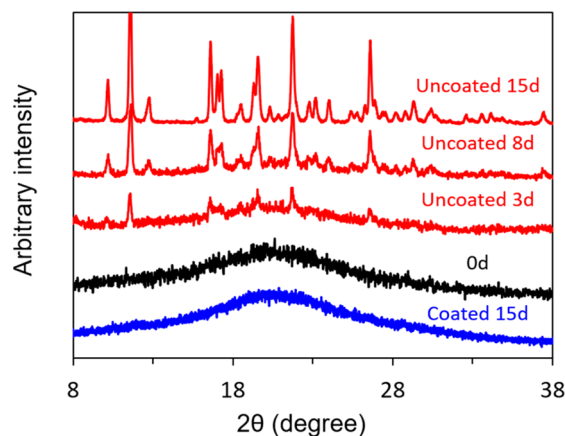


**Figure 2.** X-ray diffraction patterns of uncoated and chitosan-coated amorphous IMC particles at time zero and after specified times at 30 °C and 75% RH. Uncoated particles showed significant crystallization, while coated particles remained amorphous.

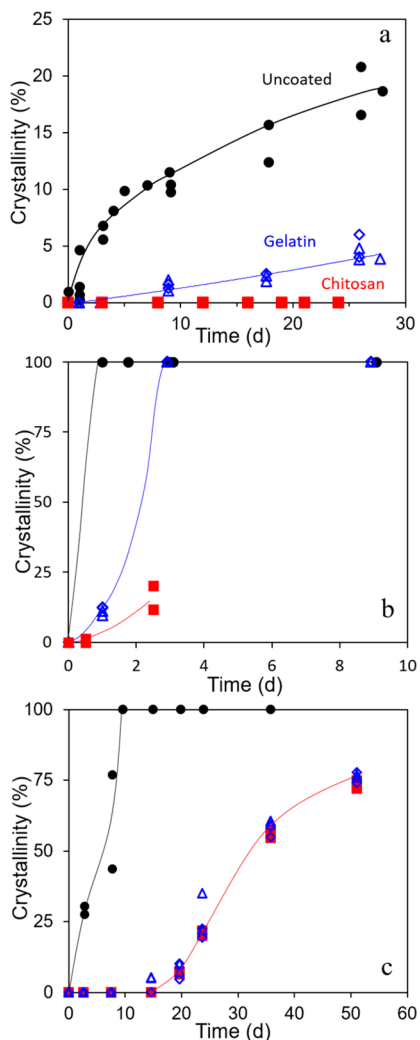


**Figure 3.** Effect of chitosan coating on the physical stability of amorphous IMC particles under different conditions: (a) 40 °C and dry (0–5% RH), (b) 40 °C and 75% RH, (c) 30 °C and 75% RH. Black circles: uncoated particles. Blue open triangles: gelatin-A-coated particles. Blue open diamonds: gelatin-B-coated particles. Red squares: chitosan-coated particles.

density of chitosan relative to gelatin, enabling stronger ionic interactions between chitosan and IMC.

The data in Figure 3 show that moisture can greatly accelerate the crystallization process even under a polymer coating. Uncoated particles remain mostly amorphous after 30 days at 40 °C under a dry condition, but at 40 °C and 75% RH, crystallization is complete in 1 day. This effect has been reported previously and attributed to increased molecular mobility in the presence of absorbed moisture.<sup>13,14</sup> Our polymer coating is extremely thin (several nanometers), and chitosan is hydrophilic in nature. Such a coating is not expected to prevent the entry of moisture into the amorphous drug. Future work could investigate other polymer systems to learn whether performance under humid conditions can be improved.

**Comparison of Particle Formation Methods.** As described in the Materials and Methods Section, several methods were used to prepare coated amorphous particles. These methods differ in terms of energy input and particle formation; they are expected to cause different degrees of in-process crystal nucleation and produce particles with different stability on storage. In Figure 4, we compare the rates of

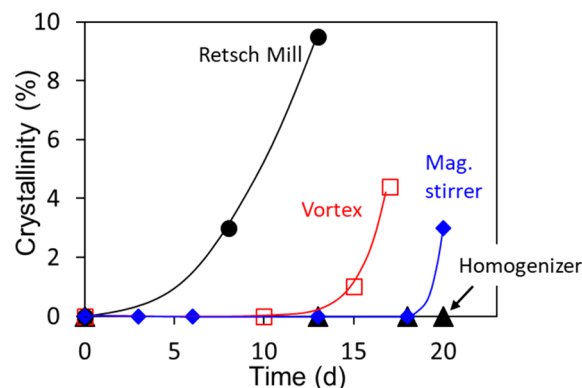


**Figure 4.** Stability of particles prepared by different methods at 40 °C. The particles prepared by the homogenizer method show the best stability against crystallization.

crystallization of coated amorphous particles prepared by different methods. With all the methods used, the as-prepared particles were amorphous according to XRD. At 40 °C, particles prepared by the homogenizer method remained amorphous for at least 20 days, while particles prepared by the other methods all crystallized faster. This result suggests that among the four methods under the conditions used, the homogenizer method performed the best. This is possibly a result of its efficient mixing and low energy input during particle formation.

**Dissolution Rate.** Figure 5 shows the effect of chitosan coating on the dissolution rate of amorphous IMC particles. To be able to compare our results with the previous results on uncoated particles,<sup>15,16</sup> we performed dissolution measurements in unbuffered Milli-Q water. As a point of reference, we also measured the dissolution kinetics of uncoated crystalline IMC particles ( $\gamma$  polymorph) under the same condition. The plateau concentration of 8.5  $\mu\text{g}/\text{mL}$  reached by the crystalline particles corresponds to the solubility of  $\gamma$  IMC, which agrees with the result of Hancock and Park (5  $\mu\text{g}/\text{mL}$  at 25 °C and 12  $\mu\text{g}/\text{mL}$  at 45 °C).<sup>15</sup> For the uncoated amorphous particles, we observed faster dissolution rate relative to the uncoated

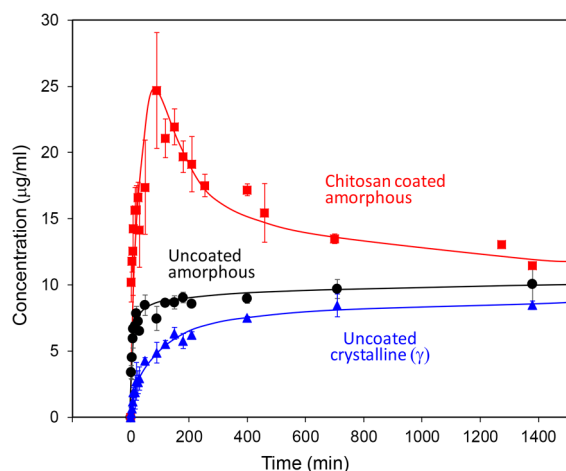


**Figure 5.** Effect of chitosan coating on the dissolution rate of amorphous IMC particles at 37 °C. Each data point shown is the average of three independent measurements.

crystalline particles, in agreement with the previous reports.<sup>15,16</sup> Note, however, the dissolution profile of our uncoated amorphous particles (Figure 5) is missing a transient concentration peak seen in previous studies.<sup>15,16</sup> This is attributed to a lower particle loading into the dissolution vessel, as discussed below. Over time, the solution concentration reached by uncoated amorphous particles approaches the crystal solubility, indicating that the amorphous particles crystallized during testing. This was confirmed by postdissolution XRD analysis and by the color change of the IMC powder from yellow to white; it is also consistent with the previous interpretation of the amorphous IMC dissolution kinetics.<sup>15,16</sup> It is noteworthy that the solution concentration reached by uncoated amorphous particles approaches the crystal solubility but within the time of observation does not quite attain it. This may be due to incomplete crystallization and/or crystallization to a different polymorph.<sup>15,16</sup> In contrast to uncoated amorphous particles, chitosan-coated amorphous particles show a significantly enhanced dissolution rate, producing a peak concentration that lasts for several hours, which gradually decreases in the course of 1 day.

The enhanced dissolution of chitosan-coated particles is attributed to improved wetting and prevention of crystallization. During the dissolution test, chitosan-coated particles



were observed to circulate freely in the dissolution medium with stirring, whereas uncoated or crystalline particles tended to float on the surface. A derivative of cellulose, chitosan is more hydrophilic than indomethacin. Thus, coated particles are more easily wetted by water, which increases the dissolution rate. It is also noteworthy that the dissolution of uncoated amorphous particles did not create a peak concentration (the “spring effect”). This is because the uncoated particles crystallized quickly on contact with water, resulting in a solution concentration that is close to the crystal solubility (Figure 5). In contrast, coated amorphous particles show a peak concentration around 100 min, which “parachutes” down gradually in the course of 1 day. This indicates that a chitosan coating delayed the crystallization process, allowing the solution to reach and sustain high supersaturation.

In the case of uncoated amorphous particles, previous workers observed a peak concentration during dissolution,<sup>15,16</sup> but this peak is absent in our result (Figure 5). We attribute this difference to the *amount* of the particles loaded into the dissolution vessel. The previous workers used a loading level of 2 mg/mL, while our loading level was much lower (0.25 mg/mL), chosen to represent the pharmaceutical condition for an oral dosage form. Presumably, at a higher particle loading, the total surface area of amorphous particles is larger, leading to a higher flux of dissolved molecules into the solution and creating a more pronounced peak in the concentration vs time profile.

**Powder Flow.** Table 1 compares the flowability of uncoated and coated IMC particles in two different ways. First, the angle of repose is significantly smaller for chitosan-coated particles, indicating better flowability. Second, the flowability indices ( $ff_c$ ) indicate that the uncoated powder is cohesive ( $ff_c = 4.1$ ), while the coated powder is free-flowing ( $ff_c = 10.1$ ).<sup>17</sup> This improved flowability is adequate for high-speed tableting, since the  $ff_c$  value is higher than that of microcrystalline cellulose, Avicel PH102, which flows adequately during such a process.<sup>18</sup>

The improved powder flow by polymer coating can be understood in terms of modified physical and chemical environment on the surface. A polymer coating may make a surface smoother and cover its defects and pores, as shown by the significantly reduced roughness of HPMC-coated ibuprofen particles.<sup>19</sup> It is also possible that a polymer coating reduces the cohesion between drug particles. This latter effect

**Table 1.** Comparison of the Flowability of Particles Using the Angle of Repose and Flow Function Coefficient  $ff_c$

	Uncoated	Coated
Flowability Test		
Angle of Repose, deg.	41.4 ± 3.6 (n=3)	34.5 ± 4.1 (n=3)
$ff_c$	4.1 ± 0.2 (n=3)	10.1 ± 1.9 (n=3)

is supported by the similar  $f_f$  values between chitosan (10.4) and coated IMC particles (10.1).

We observed a significant difference between gelatin and chitosan-coated particles in terms of flowability upon storage (Figure 6). After two months at 30 °C/75% RH, chitosan-



**Figure 6.** Comparison of gelatin- and chitosan-coated particles. Storage at 30 °C and 75% RH causes gelatin-coated particles to stick together and to the container, whereas chitosan-coated particles remain free-flowing.

coated particles remained free-flowing; in contrast, gelatin-coated particles stuck to each other and to the container within several days. Gelatin is known to swell and become sticky after absorbing moisture, and this may lead to poor flowability of gelatin-coated particles. With respect to both stability and flowability, chitosan is a better coating material than gelatin.

**Tabletability.** Figure 7 compares the tensile strength of tablets prepared with uncoated and coated amorphous IMC

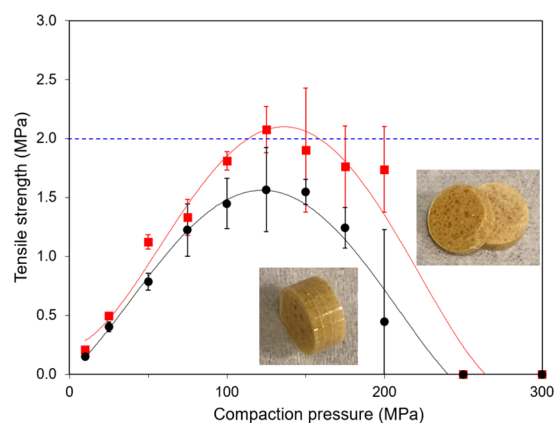


**Figure 7.** Effect of chitosan coating on the tensile strength of tablets prepared with amorphous IMC particles. Tensile strength of the tablet is plotted against compaction pressure. Black circles: uncoated particles. Red squares: chitosan-coated particles. Up to 200 MPa, the tablet of chitosan-coated particles is consistently stronger. Above this compaction pressure, the tablets are “overcompressed” and delaminated (see photo). Each data point shown is the average of three independent measurements.

particles as a function of compaction pressure. Below 200 MPa of pressure, tablets prepared with chitosan-coated IMC consistently exhibited higher tensile strength than those prepared with uncoated IMC. This indicates that even an ultrathin chitosan coating can improve the tabletability of amorphous particles. It is remarkable that, without any additional excipients, the coated amorphous particles already show acceptable tabletability, reaching 2 MPa (horizontal line)

at 125 MPa of pressure. When the compaction pressure exceeded 125 MPa, an overcompression phenomenon was observed. In this high-pressure region, the tablets delaminated upon ejection or during the diametrical breaking test, which led to a strength decrease and higher variations in measured tensile strength. No crystallization was detected by XRD as a result of compaction (see Figure S2).

A polymer coating is known to improve tabletability of poorly compressible materials, such as silica, acetaminophen, and polymer beads.<sup>20–22</sup> This effect has been attributed to a simultaneous increase of bonding strength and bonding area of polymer-coated particles. This effect may also account for the improvement of tabletability observed in this work. A key feature of this work is that the polymer coating is extremely thin (several nanometers), suggesting the potential for improving tabletability even with ultrathin polymer coatings.

## CONCLUSIONS

This work has shown that the surface crystallization of amorphous indomethacin can be inhibited by a nanocoating of a pharmaceutically acceptable polyelectrolyte, chitosan. The coating improves the physical stability against crystallization not only in the solid state but also in a dissolution medium. Chitosan-coated particles show faster dissolution, a result of better wetting and retarded crystallization. Furthermore, a chitosan coating improves powder flow and tabletability. It is worth emphasizing that a chitosan coating prepared by electrostatic deposition is extremely thin (several nanometers), and this could facilitate the preparation of stable amorphous formulations at a high drug loading.

Since coatings prepared by electrostatic deposition are extremely thin, it is useful to examine the advantages and limitations of this technology. A potential issue for any thin coating is that it could be fragile and easily damaged. This concern can be assessed from the standpoint of performance. As this and previous work<sup>3,6</sup> show, a polymer nanocoating can inhibit the growth of surface crystals on an amorphous drug. The process of crystal growth causes volume change and local stress, and the nanocoating is effective in this highly stressful environment. In addition, the coated particles were sheared during flow testing and sieved prior to stability and dissolution testing, and the mechanical stress had no detrimental effect on the coating. Finally, even in contact with a dissolution medium, the coating remained effective in slowing down drug crystallization. All these observations indicate that despite its small thickness, a polymer nanocoating can be quite strong. This is consistent with the strong ionic interactions between chitosan and IMC. In future work, nanocoating by electrostatic deposition can be explored with other pharmaceutical polymers and extended to other amorphous drugs. In addition to acidic drugs like indomethacin, basic drugs can be protonated at low pH and coated by polyanions.

## ASSOCIATED CONTENT

### Supporting Information

The Supporting Information is available free of charge on the ACS Publications website at DOI: 10.1021/acs.molpharmaceut.8b01237.

Particle size distributions of coated and uncoated materials and X-ray diffraction patterns of crystalline particles, as-coated amorphous particles, and coated amorphous particles after compaction (PDF)

## AUTHOR INFORMATION

### Corresponding Author

\*E-mail: [lian.yu@wisc.edu](mailto:lian.yu@wisc.edu)

### ORCID

Yuhui Li: 0000-0002-2043-4338

Changquan Calvin Sun: 0000-0001-7284-5334

### Notes

The authors declare no competing financial interest.

## ACKNOWLEDGMENTS

We thank the Bill and Melinda Gates Foundation for financial support, R. Teerakapibal for experimental assistance, and Niya Bowers, Phil Goliber, and Ellen Harrington for helpful discussions.

## REFERENCES

- (1) Yu, L. Amorphous Pharmaceutical Solids: Preparation, Characterization and Stabilization. *Adv. Drug Delivery Rev.* **2001**, *48* (1), 27.
- (2) Zhu, L.; Brian, C.; Swallen, S. F.; Straus, P. T.; Ediger, M. D.; Yu, L. Surface Self Diffusion of an Organic Glass. *Phys. Rev. Lett.* **2011**, *106*, 256103.
- (3) Yu, L. Surface Mobility of Molecular Glasses and Its Importance in Physical Stability. *Adv. Drug Delivery Rev.* **2016**, *100*, 3–9.
- (4) Huang, C.; Ruan, S.; Cai, T.; Yu, L. Fast Surface Diffusion and Crystallization of Amorphous Griseofulvin. *J. Phys. Chem. B* **2017**, *121*, 9463–9468.
- (5) Wu, T.; Sun, Y.; Li, N.; de Villiers, M.; Yu, L. Inhibiting Surface Crystallization of Amorphous Indomethacin by Nanocoating. *Langmuir* **2007**, *23*, 5148–5153.
- (6) Teerakapibal, R.; Gui, Y.; Yu, L. Gelatin Nano-coating for Inhibiting Surface Crystallization of Amorphous Drugs. *Pharm. Res.* **2018**, *35*, 23.
- (7) Wang, Q. Z.; Chen, X. G.; Liu, N.; Wang, S. X.; Liu, C. S.; Meng, X. H.; Liu, C. G. Protonation constants of chitosan with different molecular weight and degree of deacetylation. *Carbohydr. Polym.* **2006**, *65* (2), 194–201.
- (8) Alves, N. M.; Picart, C.; Mano, J. F. Self-Assembling and Crosslinking of Polyelectrolyte Multilayer films of Chitosan and alginate studied by QCM and IR Spectroscopy. *Macromol. Biosci.* **2009**, *9*, 776–785.
- (9) Shi, L.; Chattoraj, S.; Sun, C. C. Reproducibility of flow properties of microcrystalline cellulose—Avicel PH102. *Powder Technol.* **2011**, *212*, 253–257.
- (10) Paul, S.; Chang, S.-Y.; Sun, C. C. The phenomenon of tablet flashing — Its impact on tableting data analysis and a method to eliminate it. *Powder Technol.* **2017**, *305*, 117–124.
- (11) Fell, J. T.; Newton, J. M. Determination of tablet strength by the diametral-compression test. *J. Pharm. Sci.* **1970**, *59*, 688–91.
- (12) Musumeci, D.; Hasebe, M.; Yu, L. Crystallization of Organic Glasses: How Does Liquid Flow Damage Surface Crystal Growth? *Cryst. Growth Des.* **2016**, *16* (5), 2931.
- (13) Andronis, V.; Zografi, G. The Molecular Mobility of Supercooled Amorphous Indomethacin as a Function of Temperature and Relative Humidity. *Pharm. Res.* **1998**, *15*, 835–842.
- (14) Andronis, V.; Yoshioka, M.; Zografi, G. Effects of Sorbed Water on the Crystallization of Indomethacin from the Amorphous State. *J. Pharm. Sci.* **1997**, *86*, 346.
- (15) Hancock, B. C.; Parks, M. What is the True Solubility Advantage for Amorphous Pharmaceuticals? *Pharm. Res.* **2000**, *17*, 397–404.
- (16) Murdande, S. B.; Pikal, M. J.; Shanker, R. M.; Bogner, R. H. Solubility Advantage of Amorphous Pharmaceuticals: I. A Thermodynamic Analysis. *J. Pharm. Sci.* **2010**, *99*, 1254–1264.
- (17) Carr, R. L. Evaluating Flow Properties of Solids. *Chem. Eng.* **1965**, *18*, 163–169.
- (18) Sun, C. C. Setting the bar for powder flow properties in successful high speed tableting. *Powder Technol.* **2010**, *201*, 106–108.
- (19) Genina, N.; Rääkkönen, H.; Ehlers, H.; Heinämäki, J.; Veski, P.; Yliruusi, J. Thin-coating as an Alternative Approach to Improve Flow Properties of Ibuprofen Powder. *Int. J. Pharm.* **2010**, *387*, 65–70.
- (20) Shi, L.; Sun, C. C. Transforming Powder Mechanical Properties by Core/Shell Structure: Compressible Sand. *J. Pharm. Sci.* **2010**, *99*, 4458–4462.
- (21) Shi, L.; Sun, C. C. Overcoming poor tableability of pharmaceutical crystals by surface modification. *Pharm. Res.* **2011**, *28*, 3248–3255.
- (22) Osei-Yeboah, F.; Sun, C. C. Tableability modulation through surface engineering. *J. Pharm. Sci.* **2015**, *104*, 2645–2648.